An Adaptive Wide-Area Load Shedding Scheme Incorporating Power System Real-Time Limitations

Tohid Shekari, *Student Member, IEEE*, Amin Gholami, *Student Member, IEEE*,
Farrokh Aminifar, *Senior Member, IEEE*, and Majid Sanaye-Pasand, *Senior Member, IEEE*

***Abstract*—Under frequency load shedding (ULFS) schemes are devised to help power system maintain the load-generation balance by shedding adequate loads to match the generation. In this paper, a new centralized adaptive load shedding scheme is proposed in three stages. The first stage determines the requirements needed for implementation of the proposed scheme. The optimal amount and location of load drops and post load shedding strategies are specified in the second stage. In addition to consideration of operational limitations and voltage stability criteria, this stage takes the interruption cost of dropped loads into account. In the third stage, the event type is determined in real time and the pre-specified optimal load shedding scheme and post load shedding strategies associated with the event are implemented. The proposed methodology is successfully testified in the IEEE 39-bus system through several case studies.**

***Index Terms*—Adaptive load shedding scheme, interruption cost, power system protection, under frequency load shedding (UFLS), voltage instability.**

NOMENCLATURE

Indexes

i, k	Indices of buses.
m_i	Index of feeders at bus i.
s	Index of solutions.

Parameters

$G_{i,k}, B_{i,k}$	Real and imaginary parts of (i, k) element of bus admittance matrix.
M	A large positive number.
P^{shed}	Total amount of load to be shed.
$\bar{P}^{l}_{i,k}$	Maximum active power flow of branch between buses i and k.
$P^{D}_{i,m_i}, Q^{D}_{i,m_i}$	Total active and reactive power demands at bus i and feeder m_i.
P^{G}_{i}, Q^{G}_{i}	Total active and reactive power generations at bus i.
$PF^{PZ}_{i,m_i}, PF^{PI}_{i,m_i}, PF^{PP}_{i,m_i}$	Participation factors of impedance-constant, current-constant, and power-constant terms in active power loads at bus i and feeder m_i.
$PF^{QZ}_{i,m_i}, PF^{QI}_{i,m_i}, PF^{QP}_{i,m_i}$	Participation factors of impedance-constant, current-constant, and power-constant terms in reactive power loads at bus i and feeder m_i.
q_i	Number of steps in the compensator bank at bus i (integer parameter).
Q^{PC}_{i}	Total reactive power of the compensator at bus i.
$R^{l}_{i,k}, X^{l}_{i,k}$	Resistance and reactance of branch between buses i and k.
$t-, t+$	Time instants immediately prior to load shedding, immediately after it.
t^*	Time instant associated with the steady-state condition.
V_i	Voltage magnitude at bus i.
$\bar{V}_i, \underline{V}_i$	Maximum and minimum limits of V^*_i.
η	Coefficient used in LRI_s.
λ_{i,m_i}	Value of lost loads (VOLL) at bus i and feeder m_i.
ξ	Accepted deviation of active power balance.

Variables

C_{i,m_i}	Interruption cost of loads at bus i and feeder m_i.
E_i	The number of energized steps of compensator at bus i $(0, 1, \ldots, q_i)$.
f_t	System frequency at the instant t.
LRI_s	Load rejection index (LRI) of solution s.
PVI_s	*P–V* margin index of solution s.
$P^{0}_{s}, P^{\max}_{s}$	Operating and critical points of *P–V* curve of solution s.
$P^{D^*}_{i,m_i}, Q^{D^*}_{i,m_i}$	Steady-state active and reactive power demands at bus i and feeder m_i after load shedding.
$P^{l}_{i,k}$	Active power flow of the branch between buses i and k.
t^{fault}, t^{osc}	Contingency occurrence time and network oscillation damping time.
V^{t-}_{i}, V^{t+}_{i}	Voltage magnitude at bus i at time instants $t-$ and $t+$.
V^{*}_{i}	Steady-state voltage magnitude after load shedding at bus i.

Manuscript received September 07, 2015; revised November 16, 2015; accepted February 20, 2016. Date of publication April 14, 2016; date of current version March 23, 2018.

The authors are with the School of Electrical and Computer Engineering, College of Engineering, University of Tehran, Tehran 11365-4563, Iran (e-mail: t.shekari@ut.ac.ir; a.gholami@ut.ac.ir; faminifar@ut.ac.ir; msanaye@ut.ac.ir).

Digital Object Identifier 10.1109/JSYST.2016.2535170

X_{i,m_i}	Binary decision variable indicating load shedding status at bus i and feeder m_i.
$\alpha_{i,m_i}, \beta_{i,m_i}$	Auxiliary continuous variables.
Δt	Simulation time step (1 ms).
ε	Minimum acceptable value for frequency oscillations.
$\varphi_{i,k}$	Difference of steady-state voltage angles between buses i and k.
$\omega_{i,k}$	Piecewise linear approximation of $\cos(\varphi_{i,k})$.

I. Introduction

BLACKOUTS, although happen infrequently, cause vast social and economic damages [1]. In recent years, many researchers have investigated the origins of blackouts. As it has been revealed by these studies, voltage collapse and large frequency diminution are two adverse phenomena that can cause major disturbances in power networks [1]. Under specific circumstances (e.g., during a pure voltage decrease or in small disturbances), voltage stability and frequency diminution can be studied independently. However, in the case of severe contingencies, there is a strong relationship between voltage instability and high frequency decline [2].

Although it seems to be impossible to eliminate all blackouts due to some natural and unpredictable events and human errors, some efforts can be stepped up in order to reduce the duration and number of interruptions using new methods and technologies [1]. One of the most effective ways to face severe disturbances in power systems is accommodating special defensive measures commonly referred to as "defense plans" [3]. The defense plan could be considered as another layer of protection system and is the last resort for maintaining system stability.

Under frequency load shedding (UFLS) scheme, as a common sort of defense plan, is the last resort to arrest declining frequency and to preserve the security of both generation and transmission systems following under-frequency events. The approach of designing a conventional local UFLS scheme, including determination of the size and number of load shedding steps and calculation of relay settings has been addressed in [4]. It goes without saying that the main disadvantage of the conventional UFLS scheme is its rigidity in dealing with different contingencies. Indeed, the loads to be shed are always constant, regardless of the location and intensity of the disturbance. Evidently, such a nonadaptive load shedding scheme cannot bring optimal outcomes. In addition, it does not consider any voltage criterion as an input to guard the system against voltage stability.

To date, several algorithms have been proposed in the literature to improve the adaptability of the conventional UFLS scheme, which can be categorized into two classes: centralized and decentralized methods. The methods proposed in [5] use local voltage and frequency signals for enhancement of power system stability. In these decentralized algorithms, load shedding is started from the buses which have higher voltage decays. The location, speed, and amount of load shedding are adjusted adaptively based on the disturbance location, the rate of frequency decline, and voltage status of the network.

In [6], two centralized load shedding algorithms are proposed for prioritizing the loads to be shed according to their voltage magnitude and VQ margins. In the centralized schemes proposed in [7] and [8], the scenario of load shedding is determined based on complete information about the power network. The advantages of these centralized schemes include accurate decision-making, more stability margins against major disturbances, and consideration of both voltage and frequency stability assessments.

This paper presents a new adaptive wide-area load shedding scheme which respects both frequency and voltage stability assessments simultaneously. The developed scheme arranges a lookup table including the optimal location and amount of load drops along with post load shedding strategies for the relevant incidents. To be adapted to real-time (RT) conditions of the network, the table is updated periodically. The proposed approach is event-based and performs relevant actions expeditiously to protect the system against the risk of blackout. Some features of the novel approach are as follows:

- recovering the frequency into the allowable range;
- minimizing the interruption cost of rejected loads;
- developing an adaptive framework satisfying RT operational limitations;
- implementation of appropriate post load shedding strategies with the purpose of preserving the system stability after the execution of load shedding;
- requiring a limited set of data;
- proposing a linear formulation to tackle computational challenges.

These features enable the new approach to act as a part of a defense plan against voltage and frequency instability risks.

II. Proposed Methodology

In the proposed load shedding scheme, decisions are made based on measurements, gathered from the power network. Snapshots of data are fed into a state estimation (SE) program. Then, an AC power flow is used to define the load shedding solution: decisions are which loads to be shed and which post load shedding strategies to be thereafter implemented (e.g., switching reactive power equipment). Deployment of post load shedding strategies could considerably protect the system against voltage collapse after implementation of load shedding. The dynamic aspects of the load shedding problem are assiduously considered through a fuzzy decision-making framework.

The new approach is executed hierarchically in three stages, i.e., requirement analysis (RA) stage, pre-disturbance preparation (PP) stage, and RT stage. Tasks of each stage are briefly presented in Fig. 1 and detailed explanations and formulations are given as follows.

A. Requirement Analysis (RA) Stage

1) Information Requirement Analysis: Many electricity industries utilize supervisory control and data acquisition (SCADA) systems to collect all the required data through substation remote terminal units (RTUs). In general, these measurements can be categorized into two groups: 1) measurands (continuous data such as active and reactive power flows) and

Stages	Tasks
Requirement analysis (RA)	• Analyze information requirements for execution of the proposed scheme and check the adequacy of the existing measurement configuration. • Sizing and placement of reactive power equipment, if necessary, in three steps, as follows: 1) perform contingencies analysis to identify trouble spots; 2) develop appropriate control strategies as supplementary corrective actions for some severe under-frequency contingencies; and 3) install specified reactive power control equipment at determined substations.
Pre-disturbance preparation (PP)	• Take snapshots of data periodically and run SE program in each period in order to monitor the power network. • Screen and rank contingencies based on the SE model. • Create a solution pool for dealing with credible contingencies. • Validate and evaluate different possible solutions by applying a set of criteria and arrange a lookup table.
Real-time (RT)	• Monitor the status of circuit breakers using indication data. • Analyze network topology and detect event type. • Shed predetermined loads according to the lookup table from the PP stage. • Perform post load shedding strategies from the PP stage.

Fig. 1. Hierarchical structure of the proposed methodology.

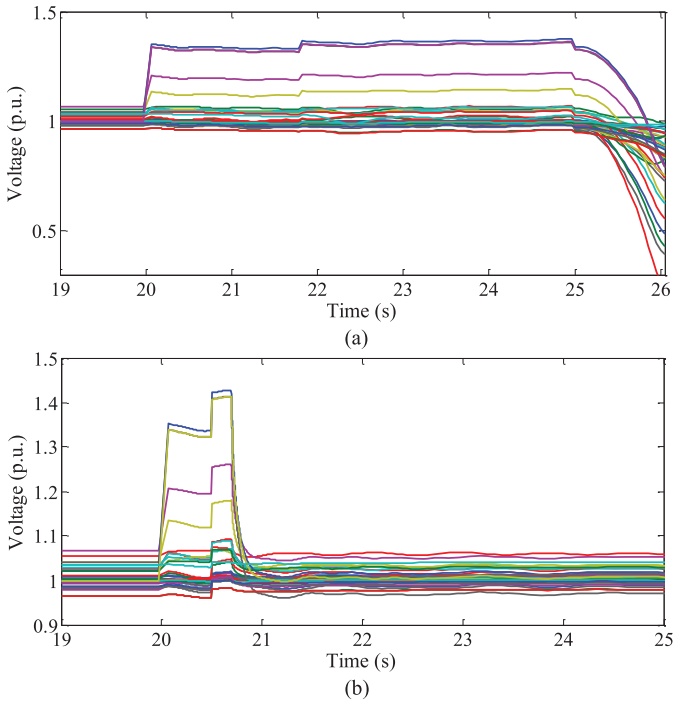

Fig. 2. Comparison of voltage profiles after the load shedding. (a) Excluding control strategy. (b) Implementation of a control strategy at 20.7 s.

2) indications (binary data including breakers' and disconnectors' status and running status of units). In common communication protocols used in power systems such as IEC 60870, indications take priority over measurands for the transmission [9]. The proposed scheme attempts to exploit this priority to handle the potential communication and data problems. Thus, indication data are employed here to directly detect the disturbances and take load shedding measures. Consequently, conventional SCADA systems satisfy the data and communication requirements.

Observability of a network is determined by the location and type of available measurements as well as by the topology of the network [10]. Here, it is assumed that a full observability of the network is ensured. However, more investigations may be carried out offline during the RA stage in order to check the adequacy of the existing measurement configuration.

2) Sizing and Placement of Supplementary Reactive Power Control Equipment: In some contingencies such as outage of a power plant or a tie-line disconnection, the system frequency returns back to the permissible range after the operation of under-frequency relays. Nevertheless, voltage instability in some buses results in system collapse. Applying appropriate post load shedding strategies could be a viable solution in these cases. The proposed scheme employs the existing reactive power control equipment in order to maintain the network stability. To do so, trouble spots of the power network are identified by performing a contingency analysis. For each under-frequency contingency, the proposed scheme attempts to preserve the network stability if the existing reactive power control equipment suffices. Otherwise, the size and location of new supplementary equipments are specified to be installed.

As an illustration, outage of generator 38 in the IEEE 39-bus system [11] leads to an overvoltage of 1.13, 1.20, 1.33, and 1.34 p.u. at buses 26, 28, 29, and 38, respectively (Fig. 2(a)). Subsequently, under-frequency relays shed 960 MW of network load (at $t = 21.7$s) which intensifies the overvoltage at the associated buses. The AVRs cannot control this phenomenon; the loads of aforementioned buses are hence rejected. To alleviate this problem, an appropriate post load shedding strategy should guarantee stability of the network after the load shedding process. Note that prior to occurrence of this contingency, generator 38 was consuming 170 MVAr and lines 28–29, 26–28, and 26–29 were in the light load condition. A passive shunt reactor at bus 28 could therefore maintain a satisfactory voltage profile for this disturbance (Fig. 2(b)). As can be seen, the proposed scheme including control strategies can find a set of solutions for such events and keep system stable against them. Detailed method and formulation of post load shedding equipment allocation for a severe contingency can be found in [12].

B. Pre-disturbance Preparation (PP) Stage

Under different operating conditions, prearranged defensive measures to face a specific perturbation may change. As a solution, the PP stage will attempt to foresee appropriate control actions associated with designated operating conditions. At every time step of T, snapshots of data are taken and SE is executed. Then, credible contingencies are screened and ranked based on the SE model. Since associated with each contingency, multiple static solutions might exist, a solution pool is created for each tackled contingency. Finally, the obtained solutions are evaluated by means of a set of dynamic criteria so as to choose the best one for implementation.

1) Formulation of the Load Shedding Scheme: In this section, the load shedding problem is formulated within

mixed-integer linear programming (MILP) format. There exist both types of continuous and binary decision variables. The developed model is tackled by CPLEX which is a powerful commercial solver providing considerable ability for solving large-scale problems. Using its solution pool feature, it is possible to collect multiple optimal and suboptimal solutions for an MILP-based model [13]. The acquired solutions are evaluated in the next step with a set of appropriate criteria and the best one (from the dynamic behavior perspective) is chosen for arranging a lookup table.

The proposed load shedding problem is formulated as follows:

$$\min \sum_i \sum_{m_i} X_{i,m_i} \cdot C_{i,m_i} \tag{1}$$

subject to

$$C_{i,m_i} = \lambda_{i,m_i} \cdot P^D_{i,m_i} \tag{2}$$

$$P^{D^*}_{i,m_i} = P^D_{i,m_i} \left[PF^{PZ}_{i,m_i} (V^*_i/V_i)^2 + PF^{PI}_{i,m_i} (V^*_i/V_i) + PF^{PP}_{i,m_i} \right] \tag{3}$$

$$Q^{D^*}_{i,m_i} = Q^D_{i,m_i} \left[PF^{QZ}_{i,m_i} (V^*_i/V_i)^2 + PF^{QI}_{i,m_i} (V^*_i/V_i) + PF^{QP}_{i,m_i} \right] \tag{4}$$

$$P^{\text{shed}} - \xi \le \sum_i \sum_{m_i} X_{i,m_i} \cdot P^{D^*}_{i,m_i} \le P^{\text{shed}} + \xi \tag{5}$$

$$P^G_i - \sum_{m_i} (1 - X_{i,m_i}) \cdot P^{D^*}_{i,m_i} = \sum_k G_{i,k} V^*_i V^*_k \cos(\varphi_{i,k}) + \sum_k B_{i,k} V^*_i V^*_k \sin(\varphi_{i,k}) \tag{6}$$

$$Q^G_i - \sum_{m_i} (1 - X_{i,m_i}) \cdot Q^{D^*}_{i,m_i} + E_i \cdot Q^{PC}_i / q_i = \sum_k G_{i,k} V^*_i V^*_k \sin(\varphi_{i,k}) - \sum_k B_{i,k} V^*_i V^*_k \cos(\varphi_{i,k}) \tag{7}$$

$$P^l_{i,k} = \frac{R^l_{i,k} (V^*_i)^2}{(R^l_{i,k})^2 + (X^l_{i,k})^2} - \frac{R^l_{i,k} (V^*_i V^*_k)}{(R^l_{i,k})^2 + (X^l_{i,k})^2} \cos(\varphi_{i,k}) + \frac{X^l_{i,k} (V^*_i V^*_k)}{(R^l_{i,k})^2 + (X^l_{i,k})^2} \sin(\varphi_{i,k}) \tag{8}$$

$$-\bar{P}^l_{i,k} \le P^l_{i,k} \le \bar{P}^l_{i,k} \tag{9}$$

$$\underline{V}_i \le V^*_i \le \bar{V}_i. \tag{10}$$

The objective of this problem (1) is to minimize the interruption cost of rejected loads subject to system operational limitations such as bus voltages and transmission line flows following the load shedding. This issue is vital to avoid the probable cascade spreading which is the main origin of large blackouts. Constraint (2) defines the interruption cost of each feeder. In this equation, λ_{i,m_i} is a socioeconomic parameter that represents the value of lost loads (VOLL) in the associated feeder. VOLL can vary for different types of loads (e.g., industrial, commercial, agricultural, residential, and general loads) in various load levels (e.g., light load, medium load, and peak load) [14].

The active and reactive power demands at different feeders are dependent on the voltage. Here, a polynomial load model is taken into account and is modeled by (3) and (4) [15]. It should be noted that in this stage, the model dependency on frequency is neglected due to the negligible deviation between the nominal and steady-state recovery frequencies. In other words, following a load shedding scenario, the system frequency returns back to near its nominal value which justifies its overlooking in (3) and (4). Nevertheless, from a dynamic viewpoint, the frequency-dependent behavior of loads is taken into account in the time-domain simulations. Participation factors of different load types (e.g., impedance-constant, current-constant, and power-constant) are obtained from offline analysis in various load levels. These factors are defined as the contribution of different load types in the total demand of each feeder.

In the process of returning the frequency back into the allowable range, the balance of active power would be recovered. Equation (5) satisfies the active power balance constraint considering an acceptable slight deviation. AC power flow equations are defined in (6) and (7). It is important to note that the appropriate control strategy for a particular event is determined by (7). In this equation, in order to recover the reactive power balance in the network, optimal energized steps of compensators installed at different buses are determined.

Active power flows of the network branches are computed in (8). Equation (9) defines the active power flow limitation for the branches. Finally, the allowable range of voltage magnitudes for different buses is taken into account in (10).

The developed load shedding model in the set of equations (1)–(10) is nonlinear. It should be linearized in order to have practical merits of MILP models associated with large-scale networks. According to a typical range of operating voltages (i.e., $0.95 \le V_i \le 1.05$ and $0.95 \le V^*_i \le 1.05$), (11) and (12) are defined as the linear model of (3) and (4) with an ignorable error. It is necessary to note that in these equations, V_i is a parameter which is obtained from SE.

$$P^{D^*}_{i,m_i} = P^D_{i,m_i} \left[PF^{PZ}_{i,m_i} (1 + 2(V^*_i - V_i)) + PF^{PI}_{i,m_i} (V^*_i/V_i) + PF^{PP}_{i,m_i} \right] \tag{11}$$

$$Q^{D^*}_{i,m_i} = Q^D_{i,m_i} \left[PF^{QZ}_{i,m_i} (1 + 2(V^*_i - V_i)) + PF^{QI}_{i,m_i} (V^*_i/V_i) + PF^{QP}_{i,m_i} \right]. \tag{12}$$

Equations (6)–(8) are replaced by piecewise approximation of AC power flow equations which are defined in the following equations [16]:

$$P^G_i - \sum_{m_i} (1 - X_{i,m_i}) \cdot P^{D^*}_{i,m_i} = \sum_k G_{i,k} (V^*_i + V^*_k + \omega_{i,k} - 2) + \sum_k B_{i,k} \cdot \varphi_{i,k} \tag{13}$$

$$Q_i^G - \sum_{m_i}(1 - X_{i,m_i}) \cdot Q_{i,m_i}^{D^*} + E_i \cdot Q_i^{\mathrm{PC}}/q_i = \sum_k G_{i,k} \cdot \varphi_{i,k} - \sum_k B_{i,k}\left(V_i^* + V_k^* + \omega_{i,k} - 2\right) \tag{14}$$

$$P_{i,k}^l = \frac{R_{i,k}^l(2V_i^* - 1)}{\left(R_{i,k}^l\right)^2 + \left(X_{i,k}^l\right)^2} + \frac{X_{i,k}^l \cdot \varphi_{i,k}}{\left(R_{i,k}^l\right)^2 + \left(X_{i,k}^l\right)^2} - \frac{R_{i,k}^l \cdot (V_i^* + V_k^* + \omega_{i,k} - 2)}{\left(R_{i,k}^l\right)^2 + \left(X_{i,k}^l\right)^2}. \tag{15}$$

Equations (13) and (14) are still nonlinear because they involve the product of a binary variable and a continuous variable (i.e., $X_{i,m_i}P_{i,m_i}^{D^*}$ in (13) and $X_{i,m_i}Q_{i,m_i}^{D^*}$ in (14)). In order to linearize such equations, $X_{i,m_i}P_{i,m_i}^{D^*}$ and $X_{i,m_i}Q_{i,m_i}^{D^*}$ are replaced by α_{i,m_i} and β_{i,m_i}, respectively. Also, the following auxiliary constraints must be added to the formulation in the process of linearization.

$$-M \cdot X_{i,m_i} \le \alpha_{i,m_i} \le M \cdot X_{i,m_i} \tag{16}$$

$$P_{i,m_i}^{D^*} - M \cdot (1 - X_{i,m_i}) \le \alpha_{i,m_i} \le P_{i,m_i}^{D^*} + M \cdot (1 - X_{i,m_i}) \tag{17}$$

$$-M \cdot X_{i,m_i} \le \beta_{i,m_i} \le M \cdot X_{i,m_i} \tag{18}$$

$$Q_{i,m_i}^{D^*} - M \cdot (1 - X_{i,m_i}) \le \beta_{i,m_i} \le Q_{i,m_i}^{D^*} + M \cdot (1 - X_{i,m_i}). \tag{19}$$

2) Evaluation of the Solutions: The solution pool acquired from the MILP solver includes a set of solutions which are different in terms of static and dynamic voltage stability behavior. Therefore, it is necessary to evaluate them with suitable indices in order to choose the most appropriate one for each contingency. The indices used for this purpose are defined as follows. Also, some other simple indices such as $V_{\min}$, $V_{\max}$, V_{mean}, and $f_{\min}$ are reported later for the sake of comparison of novel and conventional methods.

a) Load Rejection Index (LRI): When some loads at the end of a transmission line are abruptly rejected, it leads to overvoltage at the end of the line (Fig. 3). In order to consider the dynamic overvoltage during the load shedding process, LRI is defined in (20). In this equation, η is considered to be a value greater than 1 (say 2.5) in order to distinctly rank various solutions in terms of LRI. To calculate LRI, V_i^{t+} and V_i^* should be specified for each solution. V_i^{t+} denotes the voltage magnitude of bus i at the instant just after the load shedding and it is obtained from the time-domain simulations [17]. V_i^* is the post load shedding steady-state voltage magnitude of bus i which is obtained from the previous section. It is obvious that a greater LRI causes a less stress in the network. Besides accounting for network stress, the aforementioned index takes dynamic voltage stability into consideration as it includes a dynamic expression, V_i^{t+}. As it is revealed by the simulation results, there is an explanatory relation between LRI and the damping time (defined as the time for damping of the network frequency into the steady-state value). A greater LRI implies a less damping time which is synonym with the improved transient stability.

$$\mathrm{LRI}_s = -\sum_i \exp(\eta \times V_i^{t+})/V_i^*. \tag{20}$$

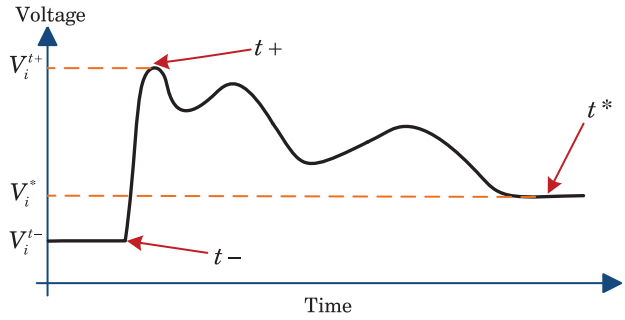

Fig. 3. Transient behavior of a bus voltage following load rejection.

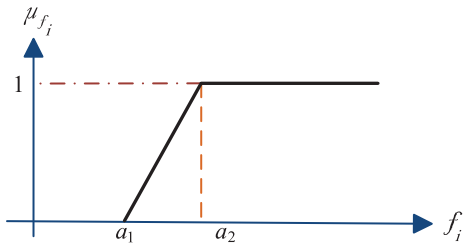

Fig. 4. Membership function for fuzzy decision-making.

b) P–V Margin Index: Voltage stability criterion illustrates how much margin is left to the voltage collapse of the system. The *P–V* curve is one of the most commonly used tools for static voltage stability analysis in power networks. In this paper, the operating and voltage stability critical points are calculated for each solution which is obtained from the solution pool process. Eventually, the following equation is used for calculating the *P–V* margin index of various solutions.

$$\mathrm{PVI}_s = \frac{P_s^0 - P_s^{\max}}{P_s^0}. \tag{21}$$

3) Fuzzy Decision-Making: The solutions obtained from the solution pool should be evaluated based on the introduced indices. Therefore, the problem is defined as a multiobjective optimization problem which maximizes the associated indices. There are several methods for solving such problems. Weighted-sum of objectives is a common method to meet this type of problems. In this method, for properly determining the weighting factors, it would need a prior knowledge of the solution. In order to mitigate the issue of weighting coefficient of each objective, we use an efficient algorithm based on fuzzy decision-making method. This approach provides an opportunity to consider the dynamic aspects of the problem, thereby choosing the solution which has the best dynamic behavior.

The procedure of fuzzy decision-making method is as follows. First, for each objective, an increasing and continuous membership function is assigned. In the maximization process, the assigned membership function for each objective is descending from a value equal to 1 at the maximum value to 0 at the minimum of the objective. A typical membership function is illustrated in Fig. 4.

In this figure, f_i and μ_{fi} stand for objective function i and the associated membership degree. a_1 and a_2 are defined as the minimum and maximum values of f_i, respectively. In the next

TABLE I
VOLL FOR VARIOUS LOAD TYPES [20]

Load type	VOLL ($/MW)	Contribution percentage (%)
General	650	16.4
Residential	190	6
Agricultural	420	23.5
Commercial	4365	11.6
Industrial	5172	42.5

step, (22) is used for determining the optimal solution of load shedding problem

$$\mu_f = \max_s \left(\min_s \left\{ \mu_s^{P-V}, \mu_s^{\text{LRI}} \right\} \right). \tag{22}$$

C. Real-Time (RT) Stage

In the last stage of the proposed structure, status of the circuit breakers is monitored continuously using the indication data. Any change in these data would trigger a topology analysis module in the control center. This module determines the type and location of the event. If the event is recognized as a severe contingency, predetermined loads would be shed based on the latest results from the PP stage. The prearranged control strategies would also be implemented simultaneously.

It is worth noting that since in the proposed method, the indication data and the load shedding trip signals are transmitted through the communication links, the communication latency should sensibly be accounted for. This aspect is discussed in the next section.

III. SIMULATION RESULTS

The proposed scheme is implemented in the IEEE 39-bus test system [11] by applying a set of realistic events. To have a more accurate survey, an eighth-order model is used for representation of generators' characteristics. In this model, the mechanical part of the generator is represented by a second-order state-space equation and the electrical part by a sixth-order system [1]. Also, the IEEE-type DC1A excitation system [18] and an appropriate governor model [19] are employed in the time-domain simulations.

Adoption of a reasonable model for representing the load dynamic behavior plays a prominent role in both voltage and frequency stability analyses. In this paper, different loads are divided into either static or dynamic categories. The static and dynamic loads are represented by the EPRI standard model and the third-order model of induction motors, respectively [5]. To have a more realistic study, load buses are divided into feeders with 20-MW active power demand. The ratio of each feeder active to reactive power demand is the same as that in the associated bus. As it can be seen in Table I, in this study, five load types are taken into account to model the interruption cost of different feeders [20].

A. Simulated Contingencies and Discussion

In this section, ten different contingencies listed in Table II are simulated in the test system. M1 and M2 denote the conventional UFLS and the proposed methods, respectively. The amount and setting of conventional UFLS relays have been designed according to [21]. Furthermore, in order to compare the new method with another wide-area adaptive approach, an advanced load shedding scheme proposed in [6] has been applied to the test system, namely M3. For evaluating the new method from different points of view, eight indices are used. The first five indices are defined to compare the steady-state behavior of three methods. In terms of voltage behavior, minimum, maximum, and mean voltages of all buses in the steady-state condition (i.e., $V_{\min}$, $V_{\max}$, and V_{mean}, respectively) are compared. Also, to appraise the results from the transient perspective, the damping time, minimum frequency of the network buses during the contingencies $f_{\min}$, and LRI are taken into account. According to [22], the less damping time results in better transient stability in the network. The indicator of damping time is defined as follows:

$$t^{\text{damping}} = t^{\text{osc}} - t^{\text{fault}} \tag{23}$$

$$t^{\text{osc}} = \min \left\{ t : |f_{t+n\Delta t} - f_t| < \varepsilon \right\}, \quad n = 1, \ldots, \frac{2.5}{\Delta t}. \tag{24}$$

Note that for each event in Table II, the symbol "–" signifies that the associated load shedding scheme cannot preserve the network stability following that event. Using the conventional UFLS scheme, following the events 1–6, the system frequency severely declines and the first step of conventional under-frequency relays is activated at 49.4 Hz. In this condition, 480 MW of network loads are dropped and the frequency returns back to its permissible range. The steady-state frequencies for these events are less than 49.9 Hz. However, owing to the substantial decrease in the reactive power generation, voltage of some buses violates the standard range (i.e., $0.95 \leq V_i^* \leq 1.05$).

Applying the proposed scheme, essential requirements of post load shedding strategies are checked. In the PP stage, different solutions are acquired to deal with the problem. Then, using the fuzzy decision-making method, the appropriate amount and location of load drops are determined. The voltage problem associated with the events 1–6 reflects that no post load shedding strategy is needed. Eventually, in the RT stage, the fault type is indicated expeditiously. As an illustration, for event 1, as soon as generator 32 fails, the breaker indication signal is sent to the control center. Therefore, the topology analyzer recognizes the event and implements the optimal load shedding according to the lookup table. In this study, in order to account for communication system latency, the total delay for implementing the load shedding is assumed to be 500 ms and the control strategy is implemented 200 ms after that. Note that according to (9) and (10), which consider the transmission capacity and voltage limitation constraints, the proposed method implements the load shedding in such a way that no transmission line is overloaded and voltage of various buses remains in the permissible range. This is vital to prevent cascading trips in a system which might eventually result in a blackout. According to the simulation results for the incidents 1–6, using the new method, the frequency returns back to its permissible range and operational limitations such as voltage of busbars and flow of branches are satisfied. In these events, even M3 cannot recover voltage magnitudes to the standard range.

TABLE II
COMPARISON OF THE SIMULATED METHODS IN DEFINED CONTINGENCIES

Event No.	Event description	Method	Load drop (MW)	Interruption cost ($)	$V_{\min}$ (p.u.)	$V_{\max}$ (p.u.)	V_{mean} (p.u.)	$f_{\min}$ (Hz)	Damping time (s)	LRI
1	Outage of generator 32	M1	480	320 000	0.84	1.0287	0.9595	49.2	95	–12.54
		M2	641	186 818	0.959	1.05	0.9946	49.77	75	–6.21
		M3	570	239 400	0.921	1.04	0.97	49.30	88	–10.02
2	Outage of the generator 36	M1	480	320 000	0.84	1.0287	0.9595	49.37	53	–3.29
		M2	522.4	136 418	0.951	1.049	1.013	49.79	32	–1.49
		M3	510	214 200	0.93	1.04	1.00	49.35	37	–2.13
3	Outage of generator 37 while lines 26–25 is out of service	M1	480	320 000	0.87	1.031	0.967	49.36	87	–9.76
		M2	509.9	127 556	0.9653	1.049	1.0013	49.75	54	–3.35
		M3	520	218 400	0.94	1.07	1.01	49.32	61	–4.52
4	Outage of generator 37 while lines 2–25 is out of service	M1	480	320 000	0.84	1.0287	0.9595	49.35	102	–14.19
		M2	501.4	128 018	0.9703	1.046	1.0259	49.75	64	–4.63
		M3	510	214 200	0.91	1.06	1.01	49.34	79	–7.81
5	Outage of generator 37 after short circuit and disconnection of lines 2–25	M1	480	320 000	0.84	1.0287	0.9595	49.2	69	–4.94
		M2	523.8	137 426	0.959	1.041	0.9934	49.78	46	–2.96
		M3	530	222 600	0.93	1.08	1.01	49.31	51	–3.17
6	Outage of generator 37 after short circuit and disconnection of lines 26–25	M1	480	320 000	0.87	1.031	0.967	49.34	61	–4.58
		M2	506.5	130 160	0.9601	1.05	0.991	49.77	37	–2.09
		M3	520	218 400	0.94	1.07	1.01	49.35	48	–3.02
7	Outage of generator 32 after disconnection of lines 21–22	M1	480	320 000	–	–	–	–	–	–
		M2	621	194 092	0.9732	1.061	1.0115	49.72	80	–7.94
		M3	650	273 000	–	–	–	–	–	–
8	Outage of generator 38	M1	960	512 000	–	–	–	–	–	–
		M2	792.2	246 626	0.9703	1.058	1.009	49.77	40	–2.17
		M3	810	340 200	0.93	1.11	1.02	49.42	53	–3.25
9	Outage of generator 38 while lines 26–29 is out of service	M1	960	512 000	–	–	–	–	–	–
		M2	790	249 356	0.9817	1.053	1.001	49.76	52	–3.23
		M3	850	357 000	0.94	1.12	1.01	49.43	65	–4.68
10	Outage of generator 38 while lines 26–28 is out of service	M1	960	512 000	–	–	–	–	–	–
		M2	790	251 498	0.9659	1.054	0.9964	49.76	68	–4.87
		M3	810	340 200	–	–	–	–	–	–

As it can be seen from Table II, the amount of load drops in M2 is more than that of M1 for the events 1–7; however, the interruption cost of rejected loads in M2 is less than that of M1. In events 1–6, shedding more loads in M2 occurs due to satisfying the network RT operational limitations (e.g., voltage of network buses and flow of transmission lines). Conversely, according to Table II, the operational limitations have not been satisfied in M1 for incidents 1–6. In the conventional case, the locations of candidate loads to be shed are fixed, despite the fact that VOLL of the different feeders changes during the day. Therefore, in the conventional case, the interruption cost of dropped loads is not optimum around-the-clock. Similarly, with regard to events 1 and 2, although in M3 the amount of load drops is less than that of M2, the operational limitations are violated using M3.

For the events 1–6, $V_{\min}$ of M1 has greatly violated, while $V_{\min}$ of M2 is in permissible range for all events. It should be noted that $V_{\max}$ of M2 has slightly violated the operating voltage range in some contingencies. This is because of the negligible linearization error, mentioned in Section II-B.

Referring to Table II, the damping time for M2 is less than that for M1 and M3. Also, greater LRI leads to less damping time in the network. That is, the greater LRI implies the improved transient stability in the system. Furthermore, owing to the fact that maximization of LRI is synonym with the minimization of voltage overshoot (see (20)), the proposed methodology seeks to minimize the voltage overshoots. In general, for the incidents 1–6, $f_{\min}$ is greater in the proposed approach due to its high speed in event indication and implementing the load drops.

In the proposed method, the amount of load drops is optimal owing to considering the network operating constraints together with employing a realistic load model in the analysis and simulations. This issue, which is suggested by the IEEE standard [23], is assiduously considered in the proposed scheme. In this way, the loads to be shed are chosen so that their shedding helps the frequency recovery not only by taking the loads as power consumers but also as entities whose behavior toward the recovered steady state plays a prominent role in the stability of the network.

For the events 7–10, the conventional method cannot maintain the network stability. For the event 7, at first a phase-to-ground short circuit occurs at $t = 19.6$ s in the middle of line 21–22 and then is cleared at $t = 19.7$ s. Following this event, generator 32 trips 300 ms later. Then, the under-frequency relays drop 480 MW of the network loads and the frequency remains in the acceptable range. In this condition, due to the considerable lack of reactive power generation, voltages at busbars around generator 32 decline substantially. Therefore, system collapse emerges due to voltage instability (Fig. 5).

Different stages of the proposed approach are applied to face this incident. Optimal load drops are acquired from the PP stage. Then, in the RT stage as indication data of line 21–22 and generator 32 are transmitted to the control center, the optimal

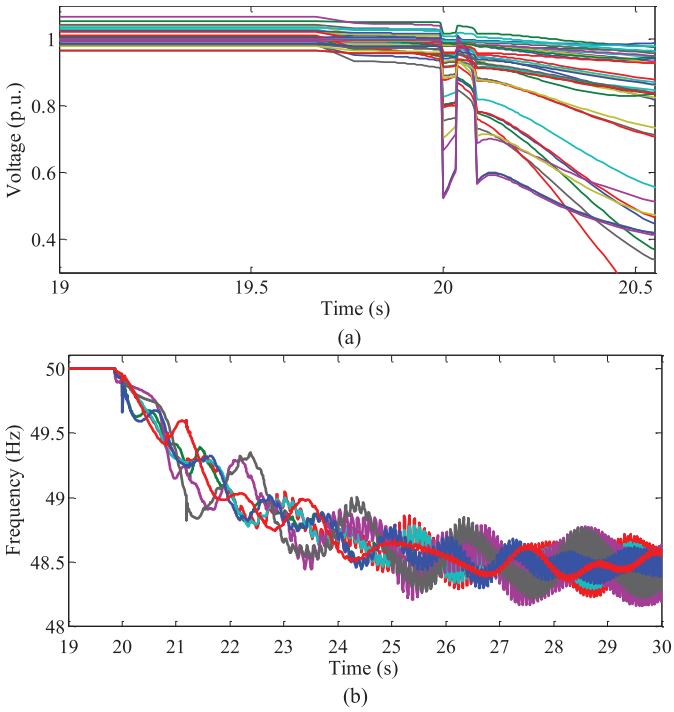

Fig. 5. Observation for the process of system collapse using conventional UFLS scheme following event 7. (a) Voltage of some busbars. (b) Bus frequency of some generators.

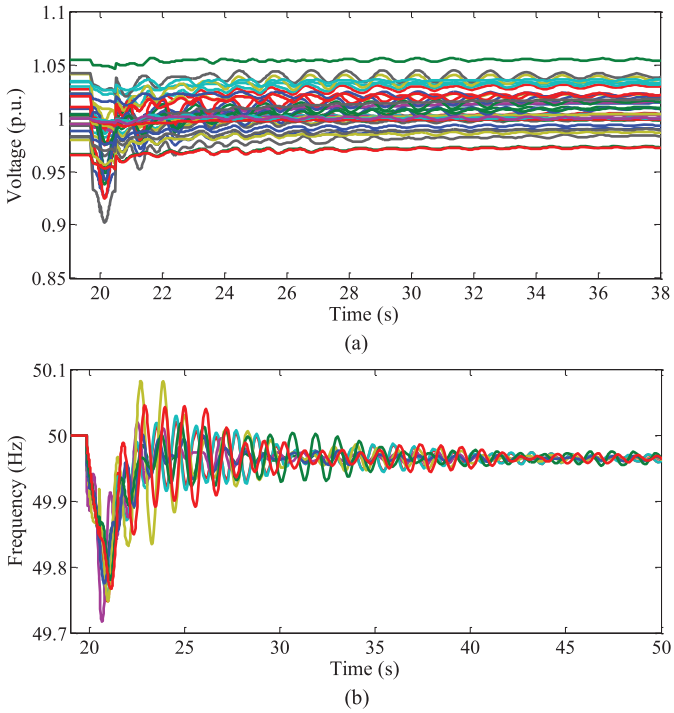

Fig. 6. Performance of the proposed scheme during event 7. (a) Voltage of some busbars. (b) Bus frequency of some generators.

load shedding is implemented in the system. Fig. 6 illustrates the performance of the new method encountering this incident. As it can be seen, the proposed method can preserve the system stability, while voltage and frequency limitations are met. For this event, no post load shedding strategy to compensate reactive power is required.

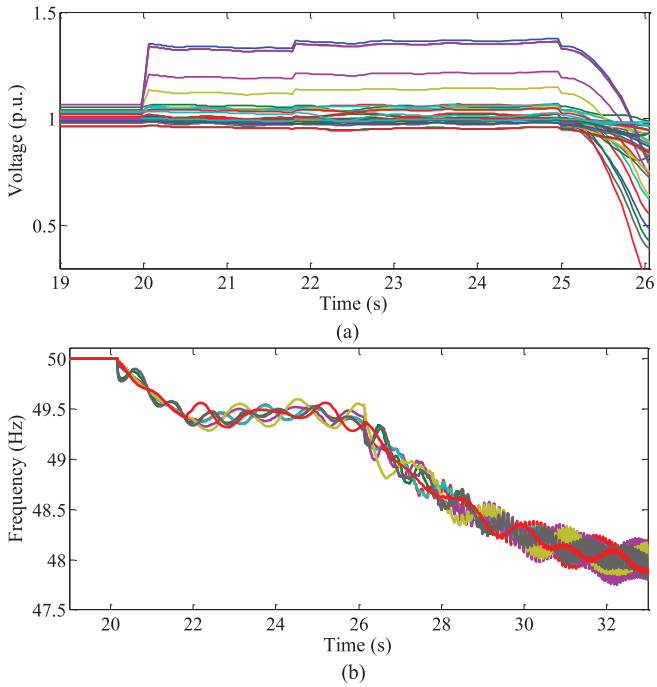

Fig. 7. Illustration of the system collapse process, as a consequence of using conventional UFLS scheme following event 8. (a) Voltage of some busbars. (b) Bus frequency of some generators.

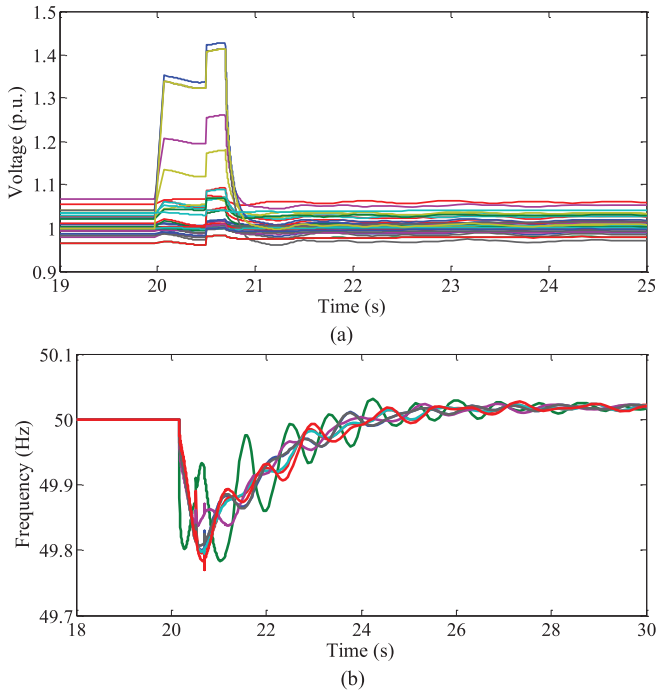

Fig. 8. Performance of the proposed scheme during the event 8. (a) Voltage of some busbars. (b) Bus frequency of some generators.

Since many researchers in the field of UFLS have confined their studies to the under-voltage phenomenon in the power networks [5], [6], here, the authors have attempted to scrutinize the overvoltage phenomenon, which is known as another source of instability. Following the incidents 8–10, steady-state overvoltage occurs at buses 26, 28, 29, and 38. Then, under-frequency relays shed 960 MW of network load which intensifies the overvoltage at the associated buses. The AVRs cannot control

this phenomenon; hence, loads of the aforementioned buses are rejected, leading to a voltage instability in the network. The required control strategy is determined for these events as discussed in Section II. The optimal solutions for load drops are obtained from the PP stage. Also, the optimum amount of the compensator installed at bus 28 should be energized to preserve the system stability against these incidents. The simulation results demonstrate that using the proposed scheme, network operational limitations are safely satisfied. An illustrative comparison between the conventional and proposed methods in an overvoltage case is presented in Figs. 7 and 8. These results prove that the proposed method is capable of preserving the system from collapsing and moving it to a new steady state and stable condition.

IV. Conclusion

To overcome the weaknesses of existing load shedding methods, a new adaptive scheme based on a hierarchical structure has been proposed in three stages in this paper. The strategic framework of the new approach brings about less communication requirements which is one of the most tremendous challenges in the centralized methods. The novel scheme has been examined on the IEEE 39-bus system through severe disturbances. Considering both voltage and frequency stability assessments along with the operational limitations have ensured that the proposed scheme will maintain the system stability while avoiding the initiation of subsequent incidents after the load rejection. Moreover, the interruption cost of dropped loads has been taken into account for having the load shedding process in an economical way. Since the proposed method is formulated as a linear problem, it is fast enough to be implemented in large-scale networks. Also, using the proposed approach, damping time of network oscillations was minimized along with maximization of LRI. Future studies could investigate the ways for decentralized implementation of load shedding schemes, possibly through the use of agent-based approaches. Furthermore, in order to have practical merits in the case of large-scale systems, the network can be partitioned into several areas and the proposed method can be implemented in each area independently.

References

[1] M. Eremia and M. Shahidehpour, *Handbook of Electrical Power System Dynamics: Modeling, Stability, and Control*. Hoboken, NJ, USA: Wiley, 2013.

[2] K. Brand, V. Lohmann, and W. Wimmer, "Wide-area protection," in *Substation Automation Handbook*, 1st ed. Bremgarten, Switzerland: Utility Automation Consulting Lohmann, 2003, pp. 214–278.

[3] M. Begovic *et al.*, "Defense plan against extreme contingencies," CIGRE Task Force C2.02.24M., Tech. Brochure, Apr. 2007.

[4] W. A. Elmore, *Protective Relaying Theory and Application*. Coral Springs, FL, USA: ABB Power T&D Company Inc., 1995.

[5] A. Saffarian and M. Sanaye-Pasand, "Enhancement of power system stability using adaptive combinational load shedding methods," *IEEE Trans. Power Syst.*, vol. 26, no. 3, pp. 1010–1020, Aug. 2011.

[6] H. Seyedi and M. Sanaye-Pasand, "New centralized adaptive load shedding algorithms to mitigate power system blackouts," *IET Gener. Transmiss. Distrib.*, vol. 3, no. 1, pp. 99–114, Jan. 2009.

[7] J. Tang, J. Liu, F. Ponci, and A. Monti, "Adaptive load shedding based on combined frequency and voltage stability assessment using synchrophasor measurements," *IEEE Trans. Power Syst.*, vol. 28, no. 2, pp. 2035–2047, May 2013.

[8] T. Shekari, F. Aminifar, and M. Sanaye-Pasand, "An analytical adaptive load shedding scheme against severe combinational disturbances," *IEEE Trans. Power Syst.*, vol. 31, no. 5, pp. 4135–4143, Sep. 2016.

[9] G. Clarke, D. Reynders, and E. Wright, *Practical Modern SCADA Protocols: DNP3, 60870.5 and Related Systems (IDC Technology)*, 1st ed., New York, NY, USA: Elsevier, 2004.

[10] A. Abur and A. G. Esposito, *Power System State Estimation: Theory and Implementation*. New York, NY, USA: Marcel Dekker, 2004.

[11] R. D. Zimmerman and C. E. Murillo-Sanchez. (2011 Dec. 14). *MATPOWER User's Manual* [Online]. Available: http://www.pserc.cornell.edu/matpower/.

[12] W. Xu and Y. Mansour, "Voltage stability analysis using generic dynamic load models," *IEEE Trans. Power Syst.*, vol. 9, no. 1, pp. 479–493, Feb. 1994.

[13] IBM. (2009). *ILOG CPLEX 12 User's Manual* [Online]. Available: http://www.ilog.com/products/cplex/.

[14] R. Billinton and R. N. Allan, *Reliability Evaluation of Power Systems*, 2nd ed., New York, NY, USA: Plenum, 1994.

[15] IEEE Task Force on Load Representation for Dynamic Performance, "Bibliography on load models for power flow and dynamic performance simulation," *IEEE Trans. Power Syst.*, vol. 10, no. 1, pp. 523–538, Feb. 1995.

[16] A. Gholami and F. Aminifar, "A hierarchical response-based approach to the load restoration problem," *IEEE Trans. Smart Grid*, vol. 8, no. 4, pp. 1700–1709, Jul. 2017.

[17] DIgSILENT. (2011). *DIgSILENT PowerFactory User's Manual* [Online]. Available: http://www.digsilent.com/.

[18] P. M. Anderson and A. A. Fouad, *Power System Control and Stability*. Piscataway, NJ, USA: IEEE Press, 1994.

[19] IEEE Committee Report, "Dynamic models for steam and hydro turbines in power system studies," *IEEE Trans. Power App. Syst.*, vol. PAS-92, no. 6, pp. 1904–1915, Nov./Dec. 1973.

[20] R. Billinton and P. Wang, "Distribution system reliability cost/worth analysis using analytical and sequential simulation techniques," *IEEE Trans. Power Syst.*, vol. 13, no. 4, pp. 1245–1250, Nov. 1998.

[21] A. P. Ghaleh, M. Sanaye-Pasand, and A. Saffarian, "Power system stability enhancement using a new combinational load shedding algorithm," *IET Gen. Transmiss. Distrib.*, vol. 5, no. 5, pp. 551–560, May 2011.

[22] M. Reza, "Stability analysis of transmission systems with high penetration of distributed generation," Ph.D. dissertation, Elect. Eng., Delft Univ. Technol., Delft, The Netherlands, Dec. 2006.

[23] *IEEE Guide for the Application of Protective Relays Used for Abnormal Frequency Load Shedding and Restoration*, IEEE Standard C37. 117–2007, Aug. 2007.

Tohid Shekari (S'14) received the B.Sc. degree in the electrical engineering from Iran University of Science and Technology, Tehran, Iran, in 2013. He is currently working toward the M.Sc. degree at the University of Tehran, Tehran, Iran.

His current research interests include power system optimization and application of wide-area measurements in power system stability and control.

Amin Gholami (S'14) received the B.Sc. (Hons.) degree in electrical engineering from Iran University of Science and Technology, Tehran, Iran, in 2013. He is currently pursuing the M.Sc. degree at the University of Tehran, Tehran, Iran.

His research interests include power system optimization and resilience.

Farrokh Aminifar (S'07–M'11–SM'15) has been collaborating with the Robert W. Galvin Center for Electricity Innovation with the Illinois Institute of Technology, Chicago, IL, USA. He is currently an Assistant Professor with the School of Electrical and Computer Engineering, the University of Tehran, Tehran. His research interests include wide-area measurement systems and smart grid initiatives.

Majid Sanaye-Pasand (M'98–SM'05) received the B.Sc. degree from the University of Tehran, Tehran, Iran, and the M.Sc. and Ph.D. degrees from the University of Calgary, Calgary, AB, Canada.

Currently, he is a Professor with the School of Electrical and Computer Engineering, the University of Tehran. His areas of interest include power system analysis and control and digital protective relays.